Inhibition of 3-D Tumor Spheroids by Timed-Released Hydrophilic and Hydrophobic Drugs from Multilayered Polymeric Microparticles

*Wei Li Lee, Wei Mei Guo, Vincent H. B. Ho, Amitaksha Saha, Han Chung Chong, Nguan Soon Tan, Effendi Widjaja, Ern Yu Tan, and Say Chye Joachim Loo**

First-line cancer chemotherapy necessitates high parenteral dosage and repeated dosing of a combination of drugs over a prolonged period. Current commercially available chemotherapeutic agents, such as Doxil and Taxol, are only capable of delivering single drug in a bolus dose. The aim of this study is to develop dual-drug-loaded, multilayered microparticles and to investigate their antitumor efficacy compared with single-drug-loaded particles. Results show hydrophilic doxorubicin HCl (DOX) and hydrophobic paclitaxel (PTX) localized in the poly(dl-lactic-co-glycolic acid, 50:50) (PLGA) shell and in the poly(l-lactic acid) (PLLA) core, respectively. The introduction of poly[(1,6-bis-carboxyphenoxy) hexane] (PCPH) into PLGA/PLLA microparticles causes PTX to be localized in the PLLA and PCPH mid-layers, whereas DOX is found in both the PLGA shell and core. PLGA/PLLA/PCPH microparticles with denser shells allow better control of DOX release. A delayed release of PTX is observed with the addition of PCPH. Three-dimensional MCF-7 spheroid studies demonstrate that controlled co-delivery of DOX and PTX from multilayered microparticles produces a greater reduction in spheroid growth rate compared with single-drug-loaded particles. This study provides mechanistic insights into how distinctive structure of multilayered microparticles can be designed to modulate the release profiles of anticancer drugs, and how co-delivery can potentially provide better antitumor response.

1. Introduction

The use of single chemotherapeutic drug (monotherapy) has shown limitations, such as low drug efficacy and the development of drug resistance in cancer therapy. The combination of two or more therapeutic agents provides a means to achieve a synergistic effect at lower drug doses.[1,2] Theoretically, therapeutic efficacy is maximized and drug resistance is less likely if two anticancer drugs with different physicochemical properties and action mechanisms are delivered simultaneously to tumor cells.[3] As such, delivery systems

Dr. W. L. Lee, A. Saha, Prof. S. C. J. Loo
School of Materials Science and Engineering
Nanyang Technological University
50 Nanyang Avenue 639798, Singapore
E-mail: joachimloo@ntu.edu.sg
W. M. Guo, Dr. V. H. B. Ho
Molecular Engineering Laboratory
A*STAR, Proteos #03–13
61 Biopolis Drive 138673, Singapore
H. C. Chong, Prof. N. S. Tan
School of Biological Sciences
Nanyang Technological University
60 Nanyang Drive 637551, Singapore
Dr. E. Widjaja
45 Hindhede Walk #01–02, 587978, Singapore
Dr. E. Y. Tan
Department of General Surgery
Tan Tock Seng Hospital, 11 Jalan Tan Tock Seng
308433, Singapore

DOI: 10.1002/smll.201400536

NANO MICRO small

that incorporate different anticancer drugs have emerged to improve the approach in conventional single-agent cancer therapy. Recently, a number of formulations (e.g., micelle-based capsules, liposomes) for cancer treatments have garnered interest in delivering two or more therapeutic agents, that is, chemical drugs, siRNA, plasmid DNA or peptide.[4–7] For example, the co-delivery of the p53 gene and doxorubicin using a cationic β-cyclodextrine-polyethylenimine carrier resulted in a synergistic effect on breast tumor in vivo, by sensitizing tumor cells with aberrant p53 function to the cytotoxic effect of doxorubicin.[8] However, in such systems, the hydrophilic agents are typically left tethered to or adsorbed onto the surface of the carrier. This surface localization would result in a burst release of drugs from the surface and consequently, the occurrence of adverse effects. In other studies, micellar biodegradable carriers loaded with doxorubicin and paclitaxel were shown to induce apoptosis more effectively in tumor cells than free drugs alone.[3,9] However, these micellar nanoparticles only offer short-term release, and separate drug loading steps would add complexity to the processing of these delivery systems.[3,10] Therefore, designing commercially viable drug carriers that can simultaneously host different anticancer drugs, while controlling their individual release, remains a challenge.

The development of biodegradable polymeric microparticles for the co-delivery of two or more anticancer drugs allows sustained release of these drugs from a single administration, thus reducing the need for repeated dosing. Polymeric microparticles, as a depot formulation, would enable continuous release of drugs and ensure prolonged exposure of tumor cells to therapeutic levels of these drugs. Compared with conventional monolithic matrix-based carriers, multilayered or multi-compartmented carriers hold better promise for controlled delivery, as the latter can be structurally manipulated.[11] Such multilayered microparticles allow selective localization of drugs in specific layers; realizing a specific timed-release at different treatment periods. For instance, drugs localized within the inner cores of double-walled microspheres were shown to mitigate burst release, while providing a sustained release profile.[12] The sustained release of hydrophilic bovine serum albumin and hydrophobic cyclosporin A was also demonstrated using poly(*ortho* ester)–poly(lactic-*co*-glycolic acid) double-walled microspheres.[13] Multilayered particles can therefore offer greater versatility in controlling drug release kinetics through the manipulation of structural configurations and polymer types.

The aim of this study was to develop dual-drug-loaded, multilayered microparticles and to evaluate their antitumor efficacy compared with single-drug-loaded particles. These multilayered microparticles can be fabricated by a convenient one-step process that allows various structural manipulations, thus enabling better control of drug release kinetics. Herein, a one-step emulsion solvent evaporation technique was employed to fabricate multidrug-loaded multilayered polymeric microparticles, with each drug localized in specific polymer layers. At the same time, the drug-layer configuration and the release profiles of different drugs from double-layered microparticles comprising poly(dl-lactic-*co*-glycolic acid, 50:50) (PLGA) and poly(L-lactic acid) (PLLA) can be altered when these drug carriers are transformed from a binary-polymer to a ternary-polymer system, by adding a surface-eroding poly[(1,6-*bis*-carboxyphenoxy) hexane] (PCPH) polymer. The model anticancer drugs used in this study were hydrophilic doxorubicin HCl (DOX) and hydrophobic paclitaxel (PTX). They are amongst the most commonly used anticancer drugs for chemotherapy, particularly in the treatment of breast cancer. Clinical studies have demonstrated that incorporation of DOX and PTX increases tumor regression rates relative to the individual drugs.[14,15] The efficacy of this delivery system was subsequently tested for tumor growth inhibition against three-dimensional (3D) human breast cancer (MCF-7) spheroids.

2. Results and Discussion

2.1. Formation of Dual-Drug-Loaded, Multilayered Microparticles

PLGA/PLLA and PLGA/PLLA/PCPH microparticles were fabricated and characterized, before their drug release profiles were assessed. The scanning electron microscopy (SEM) images of non-drug-loaded and dual-drug-loaded multilayered microparticles are shown in **Figure 1**. The microparticles were spherical in shape, and particle sizes of DOX-PTX-loaded PLGA/PLLA/PCPH microparticles were 37.7 ± 9.4 μm in diameter. Particle sizes, across all the sample groups, were kept similar for unbiased comparisons. An average particle diameter of about 30 μm was chosen as it has better syringability, and is suitable in drug-delivery depot applications (e.g., post-surgical chemotherapy through intratumoral or intraperitoneal injection and cancer treatment through intramuscular injection).[16–18]

From the Raman mapping results (**Figure 2**a), it was evident that the PLGA/PLLA microparticles had a PLGA shell–PLLA core morphological structure. During fabrication, binary-phase PLGA/PLLA solution (above cloud point) was poured into an aqueous PVA solution, and the immiscible polymers immediately phase separated as coacervate droplets; coalescing with their respective polymers within the emulsion droplets.[19] A core-shell structure was obtained with a higher mass polymer (PLGA) forming the outer layer (i.e., shell), while engulfing the polymer phase (PLLA) of lower mass (i.e., core).[20,21] For PLGA/PLLA/PCPH microparticles (Figure 2b), the presence of PCPH was found to change the overall distribution of PLGA and PLLA observed for PLGA/PLLA microparticles. For this configuration, multiple distinctive layers were observed whereby PLGA still formed the shell, but now PCPH formed the second layer and PLLA the third. The core was observed to be composed of a mixture of two polymers – PCPH and PLGA, with a larger amount of PCPH distributed at the periphery, and a larger amount of PLGA localized at the innermost region of the core. Although it was reported that PLGA and PCPH are macroscopically immiscible, there remains some degree of miscibility between these two polymers,[22,23] resulting in such distribution. The scheme of the formation of a multilayered PLGA/PLLA/PCPH particle from an emulsion droplet

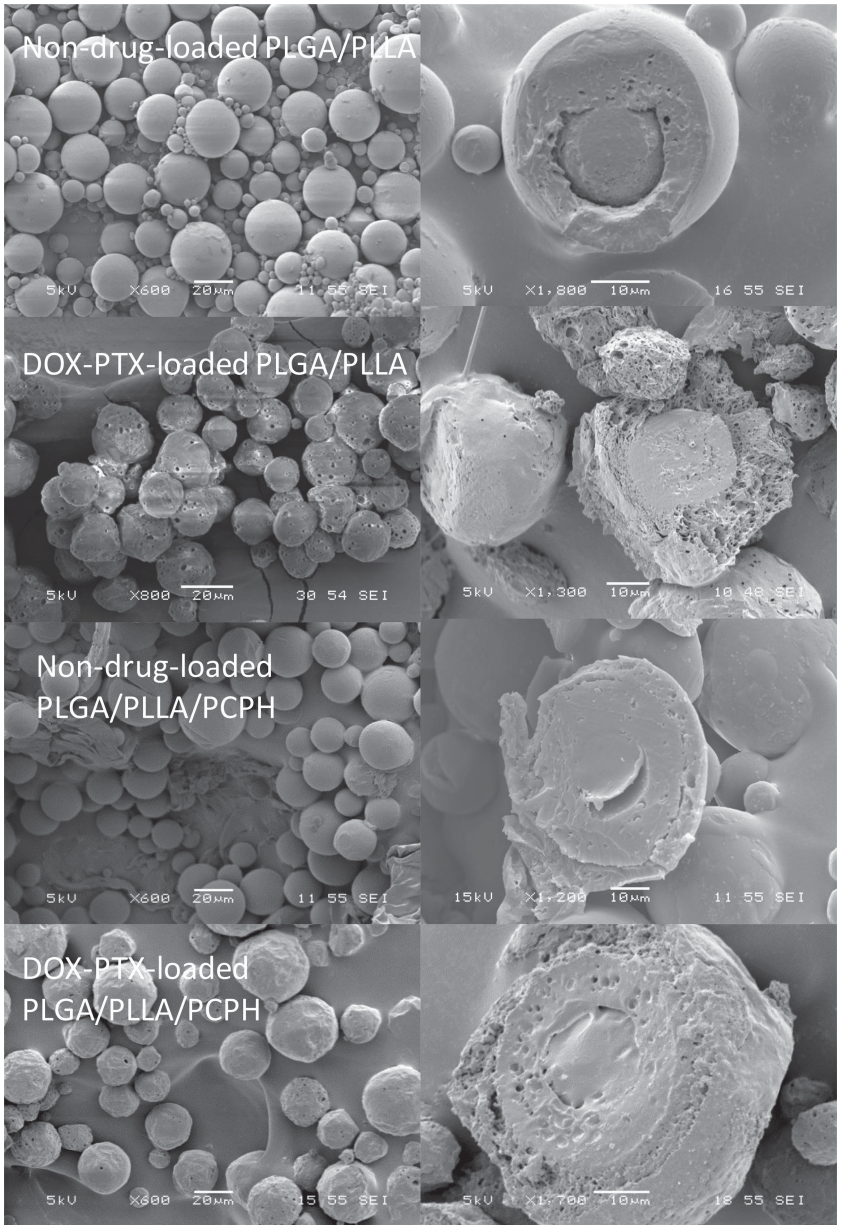

Figure 1. External and internal morphologies of the multilayered microparticles. (Row 1: Non-drug-loaded PLGA/PLLA, Row 2: DOX-PTX-loaded PLGA/PLLA, Row 3: Non-drug-loaded PLGA/PLLA/PCPH, Row 4: DOX-PTX-loaded PLGA/PLLA/PCPH).

is shown in Figure 2c. During the early stages of solvent extraction, the PLGA shell (of higher mass) predominantly consisted of PLGA and a smaller fraction of PCPH, whereas the core (the lowest polymer mass used) was predominantly composed of PCPH and a smaller amount of PLGA. When the polymer solution concentration increased (due to solvent evaporation), reaching a critical point at which the miscibility between PLGA and PCPH greatly reduced, these two polymers started to phase separate and to coalesce within their respective regions.[24] At the shell, since PCPH is relatively more hydrophobic than PLGA, PCPH would move away from the external aqueous phase, forming the second layer. At the core, the larger phase (PCPH) would therefore engulf the minor phase (PLGA). The layer configuration of PLGA/PLLA/PCPH microparticles was therefore dictated by two independent factors, that is, ratio of polymer masses and inter-miscibility of PLGA-PCPH.

Confocal laser scanning microscope (CLSM) was subsequently used to verify the localization of drugs in these multilayered microparticles. Dansyl chloride-tagged PTX (green) and fluorescent DOX (red) were used to attain a clearer visual discernment of drug localization within the microparticles. For PLGA/PLLA microparticles, specific drug localization in different layers is shown in **Figure 3**a. PTX (green) was observed in the PLLA core, while DOX (red) was in the PLGA shell. For PLGA/PLLA/PCPH microparticles, CLSM image (Figure 3b) shows that the DOX (red) was not just localized in the outermost PLGA shell, but also in the innermost core. As discussed earlier, some PLGA particulates were also embedded in the innermost core, allowing some DOX to be similarly localized in the core. Such PLGA-DOX affinity arises from hydrophilic-hydrophilic interactions, from amongst two other more hydrophobic polymers.[20,25] CLSM image (Figure 3b) also shows that PTX (green) was co-localized in both the PLLA and PCPH layers, again arising from polymer–drug affinity.[13] The images verify that highly hydrophobic PTX had preferential interactions with hydrophobic polymers (PLLA and PCPH), whereas hydrophilic DOX was distributed within the more hydrophilic PLGA.[25]

2.2. Drug Release and Degradation Mechanism of Multilayered Microparticles

The release profiles of DOX from PLGA/PLLA and PLGA/PLLA/PCPH microparticles are plotted in **Figure 4**a. PLGA/PLLA microparticles exhibited an initial burst release of DOX, of nearly 35% at day 1, whereas the release of DOX from PLGA/PLLA/PCPH microparticles was observed to be more sustained, with a highly suppressed initial burst. The differences in the release profiles can be explained from the extent of surface porosity. As observed from Figure 1, PLGA/PLLA/PCPH microparticles had a relatively dense shell, while PLGA/PLLA microparticles had a highly porous shell. A porous shell would increase water penetration, causing a rapid dissolution and release of hydrophilic DOX from the shell.[26] This porous morphology arises possibly from the leaching of hydrophilic DOX drug into the surrounding aqueous phase during the fabrication process. This phenomenon resulted in a much lower encapsulation efficiency

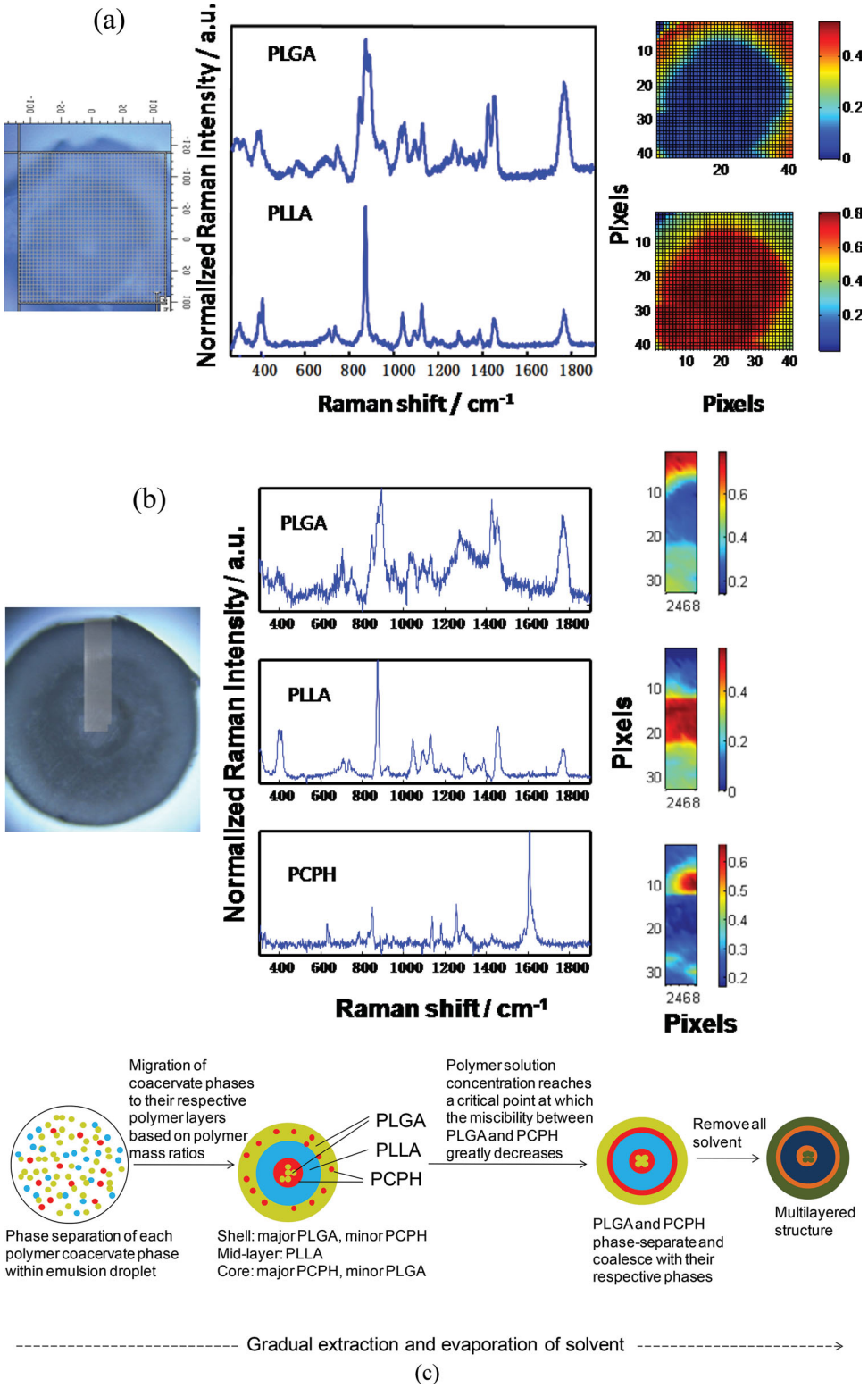

Figure 2. Pure component Raman spectra estimates and their associated score images obtained via BTEM from a) a PLGA/PLLA microparticle, b) a PLGA/PLLA/PCPH microparticle. c) Schematic illustration (not to scale) of the proposed mechanism involved in the formation of the PLGA/PLLA/PCPH microparticles.

(EE) of DOX in PLGA/PLLA microparticles, as compared with PLGA/PLLA/PCPH microparticles (**Table 1**). For PLGA/PLLA/PCPH microparticles, a denser shell together with the localization of DOX in both the shell and the innermost core aid in suppressing burst release, while providing a sustained release; with the middle layers (i.e., PLLA and PCPH) serving as diffusion barriers against its release from the core.

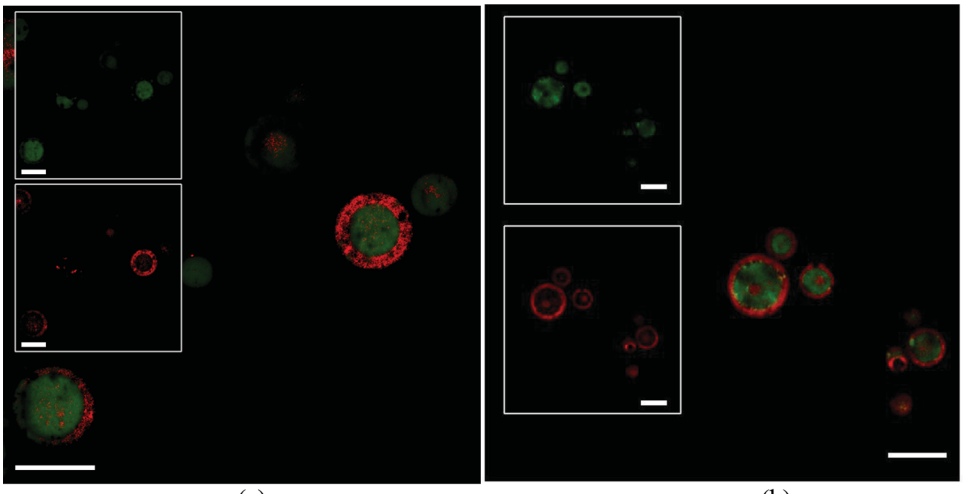

Figure 3. CLSM images of a) PLGA/PLLA microparticles and b) PLGA/PLLA/PCPH microparticles. The large images are the overlaid representation of all components. The insets are the confocal images for DOX (red) and dansyl chloride-tagged PTX (green), respectively. Scale bar = 30 μm.

For PTX, both PLGA/PLLA and PLGA/PLLA/PCPH microparticles had similarly high EE (Table 1). The release profiles of PTX from these microparticles are shown in Figure 4b. A short initial lag in the release of PTX was observed for PLGA/PLLA/PCPH microparticles. A non-porous shell along with the co-localization of PTX in both semi-crystalline PLLA and hydrophobic PCPH in PLGA/PLLA/PCPH microparticles slowed the initial release of PTX. As can be seen from the CLSM image (**Figure 5**a), PTX was still predominantly localized within the PLLA and PCPH layers even after 5 days of incubation (no observable green fluorescence in the shell). After 8 days, the release of PTX from PLGA/PLLA/PCPH microparticles proceeded more rapidly. A spread of green fluorescence along the circumferential regions of the particles suggests the diffusion of PTX (Figure 5b). From SEM images (**Figure 6**a), the morphology of PLGA/PLLA/PCPH microparticles was relatively dense at day 5, which aids in retarding the diffusion of PTX. Subsequently, the formation of pores (Figure 6b,c) together with substantial polymer degradation (Figure S1, Supporting Information) of PLGA/PLLA/PCPH particles accelerated the release of PTX. The extensive degradation of PLGA/PLLA/PCPH particles was also clearly evident from confocal imaging (Figure 5b), showing significant pore formation. The massive degradation of PLGA in the PLGA/PLLA/PCPH microparticles (Figure S1a, Supporting Information) could be attributed to acidic degradation products trapped within the relatively dense shell layer and inner core, thus accelerating the hydrolysis of PLGA (i.e., autocatalytic effect). The faster degradation of PLLA (Figure S1b, Supporting Information) with significant formation of pores in PLGA/PLLA/PCPH microparticles could be explained by the fact that the rigid aromatic rings of PCPH outer layer retarded the outward diffusion of acidic degradation products from PLLA layer, thus acid-catalyzing the degradation process.[27] As similarly reported by Pollauf et al., although PCPH is a slow degrading, surface-eroding polymer, it had been reported that the relatively thin (≈10 μm) PCPH layers could not prevent water penetration, and the degradation of inner polymer layer with the diffusion of small drug molecules could not be retarded.[22] In contrast, it was observed that PLGA/PLLA microparticles exhibited porous shells before degradation (Figure 1) and their morphology remained relatively unchanged even after 40 days of degradation (Figure 6d), thus leading to a consistent release rate of PTX. Nevertheless, it is worth mentioning that the time-delayed release obtained for PLGA/PLLA/PCPH microparticles would be beneficial for drugs that have a high first-pass effect (i.e., drugs administered for diseases with chronopharmacological behaviour), and in cases where a lag time dosing is required. The duration of this lag phase could be adjusted by tuning layer dimension and polymer degradation rates.[28,29]

The proposed mechanism for the release of DOX and PTX from microparticles is shown in **Figure 7**. Before incubation, PTX was loaded in the PLLA core surrounded by a PLGA shell loaded with DOX for PLGA/PLLA microparticles (Figure 7a, Stage I), whereas PTX was localized in both the PLLA and PCPH mid-layers and DOX was found in the PLGA shell and PLGA core for PLGA/PLLA/PCPH microparticles (Figure 7b, Stage I). By day 1, PLGA/PLLA microparticles exhibited burst release of DOX due to high porosity of the shell layer (Figure 7a, Stage II), while PLGA/PLLA/PCPH microparticles, with a relatively denser shell, suppressed any initial burst (Figure 7b, Stage II). During the latter stage (Figure 7b, Stages III-IV), the hydrophobic PLLA and PCPH middle layers served as an additional barrier for hydrophilic DOX to diffuse from the core of PLGA/PLLA/PCPH microparticles. For PTX release, during the initial period of incubation from 0 to 8 days, the dense polymer layers of PLGA/PLLA/PCPH microparticles mitigated any premature release of PTX (Figure 7b, Stages I-III). In contrast, the highly porous PLGA shell of PLGA/PLLA microparticles aided in the release of PTX (Figure 7a, Stages I-III). After 8 days of incubation, the morphology of PLGA/PLLA microparticles remained relatively unchanged (Figure 7a,

NANO MICRO small

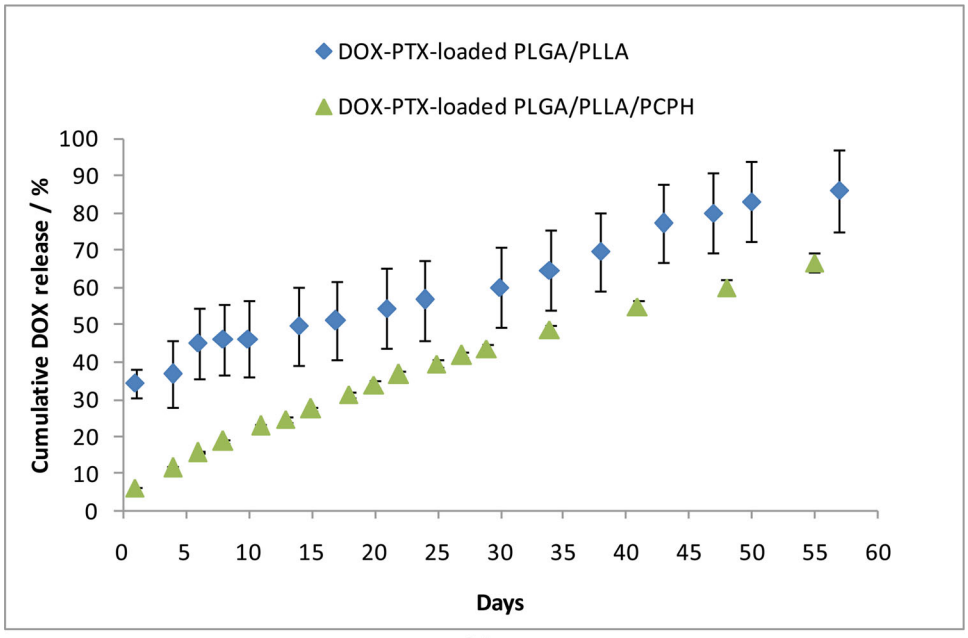

(a)

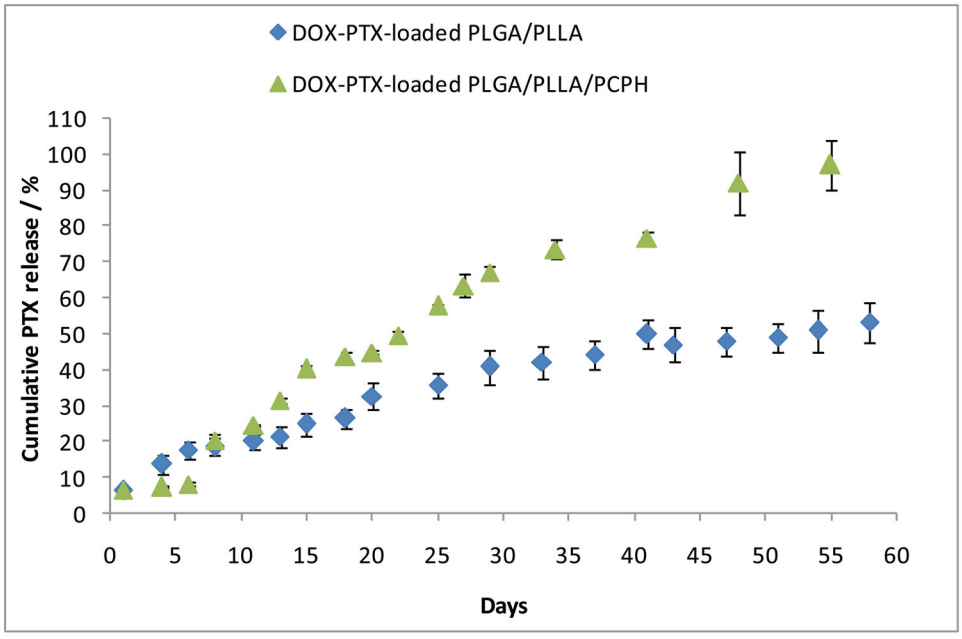

(b)

Figure 4. Release profiles of a) DOX and b) PTX from PLGA/PLLA microparticles and PLGA/PLLA/PCPH microparticles.

Stage IV), whereas PLGA/PLLA/PCPH microparticles had numerous pore formation (Figure 7b, Stage IV). Subsequent rapid degradation of PLGA/PLLA/PCPH microparticles accelerated the release of PTX after the lag phase period.

2.3. Efficacy on Three-Dimensional MCF-7 Spheroids

Drug efficacy experiments are usually conducted over 24–72 h on two-dimensional (2D) cell monolayers.[30] On the other hand, multicellular 3D spheroids provide the possibility of prolonged studies on controlled release therapeutics since they can be cultured for much longer than 72 h.[31] MCF-7 spheroids in a prolonged study of 25 days were used to elucidate the efficacy of these drug-loaded microparticles. Drug-loaded particles were able to exert an inhibitory effect on the growth of spheroids (**Figure 8**a), as compared with blank particles (without any loaded drugs). As shown in Figure 8b,

Table 1. Encapsulation efficiencies (EE) of drugs in the microparticles.

Samples	DOX [%]	PTX [%]
DOX-PTX-loaded PLGA/PLLA	21.1 ± 1.5	87.9 ± 6.9
DOX-PTX-loaded PLGA/PLLA/PCPH	48.2 ± 3.4	89.1 ± 6.1

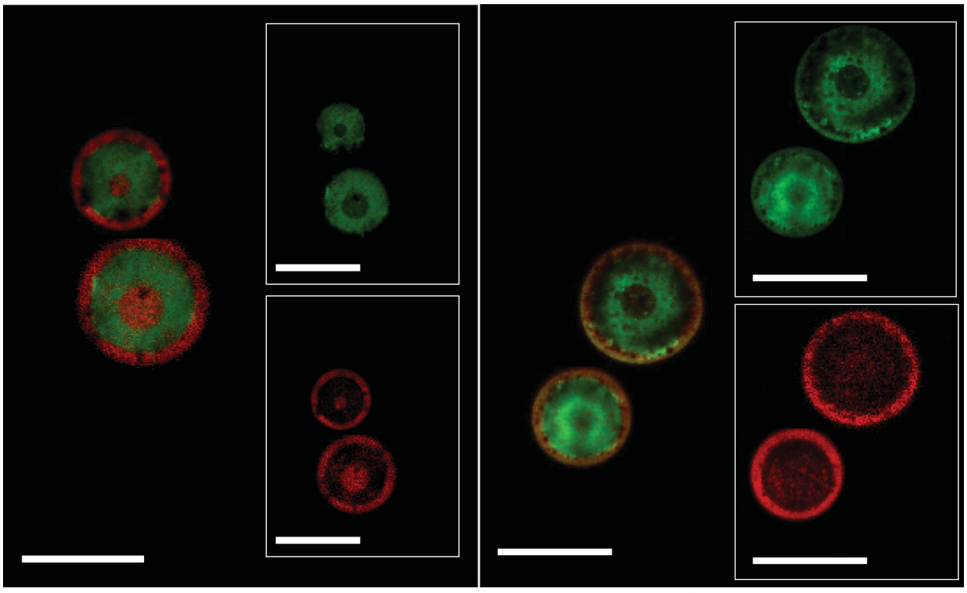

Figure 5. CLSM images depicting the distribution of drugs in the PLGA/PLLA/PCPH microparticles during the drug release process. a) After 5 days and b) after 40 days of incubation. The large images are the overlaid representation of all components. The insets are the confocal images for DOX (red) and dansyl chloride-tagged PTX (green), respectively. Scale bar = 30 μm.

co-delivery of DOX and PTX from multilayered microparticles significantly reduced spheroid growth rate, in comparison with single-drug-loaded particles ($p < 0.05$, Tukey's multiple comparison tests), demonstrating the synergistic efficacy of DOX and PTX. It is to be noted that the release profiles of single-drug-loaded microparticles resembled that of each drug from dual-drug-loaded PLGA/PLLA/PCPH microparticles (Figure S2, Supporting Information). As such, higher drug efficacy observed for dual-drug-loaded PLGA/PLLA/PCPH microparticles could be attributed to the

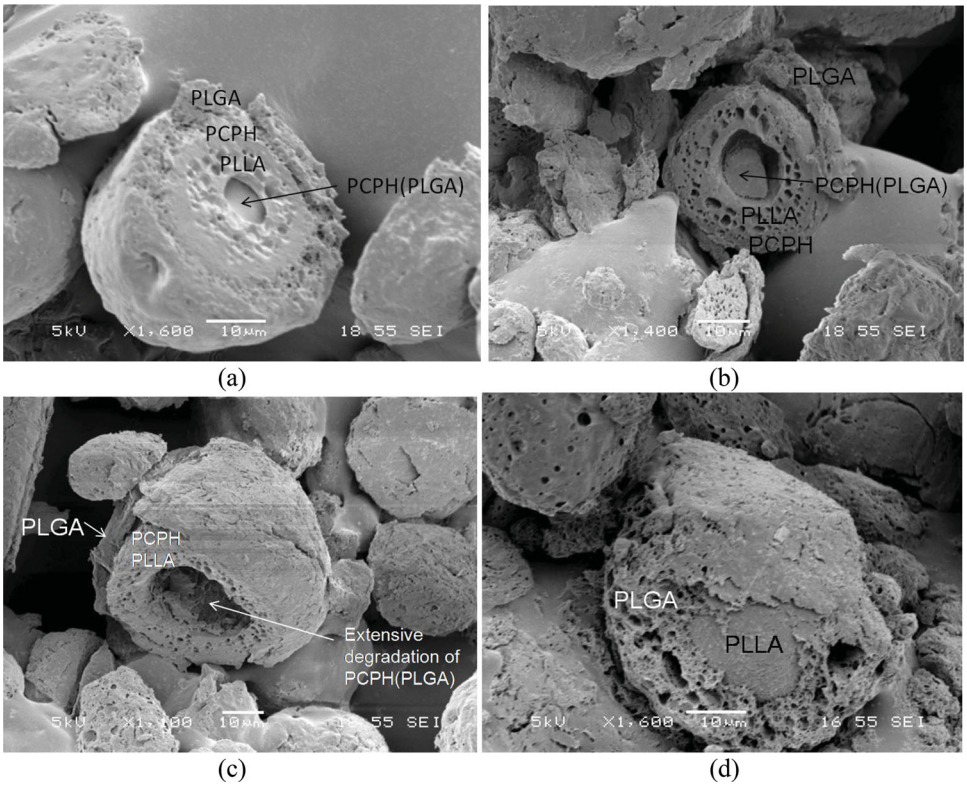

Figure 6. SEM images of the degrading DOX-PTX-loaded PLGA/PLLA/PCPH microparticles after a) 5 days, b) 12 days, and c) 40 days in vitro. d) SEM image of the degrading DOX-PTX-loaded PLGA/PLLA microparticles after 40 days in vitro.

NANO MICRO small

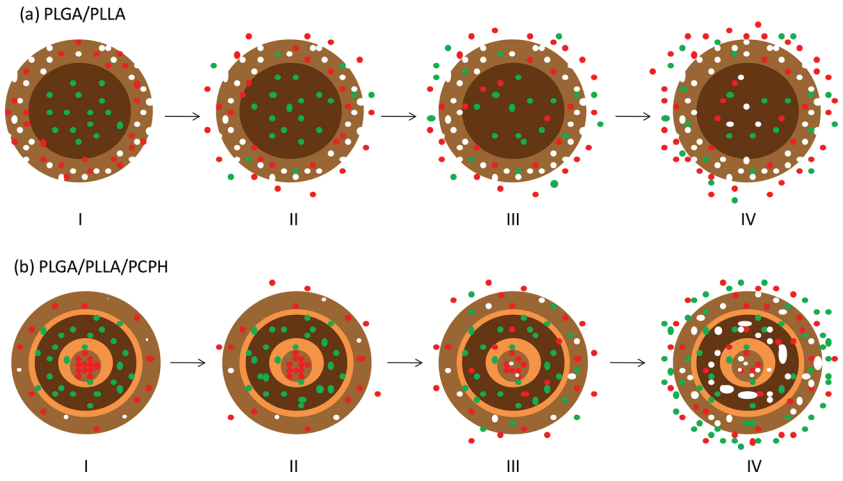

Figure 7. Schematic illustration (not to scale) of the proposed mechanism for the release of DOX and PTX from a) PLGA/PLLA and b) PLGA/PLLA/PCPH microparticles. PLGA, PLLA and PCPH are represented by light, dark brown and orange, respectively, while DOX and PTX molecules are represented by red and green dots, respectively. Stage I: Initial microparticles before degradation. Stage II: Water penetration into the microparticles. Stage III: Polymer degradation with little change in particle morphology. Stage IV: Increase in the number and size of pores of the microparticles.

complementary effect of DOX and PTX. The monitoring of spheroid volumes over the treatment duration showed that spheroids incubated with dual-drug-loaded PLGA/PLLA/PCPH microparticles exhibited a slower growth rate relative to dual-drug-loaded PLGA/PLLA microparticles (Figure 8b). This result could be attributed to the controlled and sustained release of DOX and PTX from PLGA/PLLA/PCPH microparticles. The acid phosphatase assay also indicated that the PLGA/PLLA/PCPH microparticles managed to cause a substantial decrease in overall spheroid viability at the end of the experiment (Figure 8c) due to the more substantial release of both DOX and PTX at the latter stage. One should note that although DOX- and PTX-containing media were removed from the free drug controls after short and acute free drug exposure, no significant cellular recovery was observed for these free drug treated groups. It is believed that the initial drug concentrations could be sufficient to cause significant cell death due to drugs accumulated within the spheroids during treatment.[31,32] Cells in the outer rim of spheroids usually take in most of the drugs and then undergo apoptosis. The significant apoptosis could expand interstitial space in the outer rim of spheroids, thus promoting penetration of drugs into the primed tumors.[33] The drug clearance within the spheroids could be further hindered as a result of the absence of capillaries for in vitro conditions.[34] The accumulated drugs would have almost 4 weeks to exert their cytotoxic effect, whereby PTX was reported to be more potent than DOX.[35,36] Nevertheless, it is noteworthy that administration of a relatively high initial free drug concentration or burst release from particles in vivo would likely cause serious systemic toxicity and adverse effects.[37] Since sustained and controlled drug release can be achieved with multilayered microparticles (PLGA/PLLA/PCPH), such a delivery system has the potential to increase therapeutic efficacy with minimal systemic toxicity.

3. Conclusions

Dual-drug-loaded multilayered microparticles were fabricated using a one-step emulsion solvent evaporation technique. It was found that DOX and PTX were localized in the PLGA shell and in the PLLA core, respectively. The inclusion of PCPH polymer was shown to affect the drug-layer configuration, whereby PTX was localized in both the PLLA and PCPH mid-layers and DOX was found to be in the PLGA shell and PLGA core. Release profiles of PLGA/PLLA/PCPH microparticles were compared with those of PLGA/PLLA microparticles. PLGA/PLLA microparticles yielded an initial burst release of DOX, whereas the denser shell of PLGA/PLLA/PCPH helped retard this burst. A delayed release of PTX was observed for PLGA/PLLA/PCPH, but not for PLGA/PLLA microparticles. Three-dimensional MCF-7 spheroid studies demonstrated the efficacy of drug-loaded microparticles in reducing tumor growth rate. In addition, co-delivery of DOX and PTX from multilayered microparticles showed a therapeutic advantage over single-drug-loaded particles. Multilayered microparticles may hold great promise for use in controlled delivery of multiple anticancer drugs in combination chemotherapy.

4. Experimental Section

Materials: PLLA (intrinsic viscosity (IV): 2.38, Bio Invigor), PLGA (IV: 1.18, Bio Invigor), PCPH (Aldrich) and poly (vinyl alcohol) (PVA, molecular weight (MW): 30–70 kDa, Sigma-Aldrich) were used without further purification. DOX and PTX were purchased from Xingcheng Chempharm Co. Ltd. (Zhejiang, China) and International Laboratory (USA), respectively. Dichloromethane (DCM), acetonitrile (ACN), tetrahydrofuran (THF) and chloroform from Tedia Company Inc. were of High-Performance Liquid Chromatography (HPLC) grade. Phosphate-buffered saline (PBS) solution of pH 7.4 was purchased from OHME Scientific, Singapore. Polysorbate 80 (Tween 80) was purchased from Sigma-Aldrich. Materials used for spheroid study can be found in the Supporting Information (SI).

Fabrication of Microparticles: An (oil/water) emulsion solvent evaporation method was used to prepare the PLGA/PLLA/PCPH microparticles. Briefly, polymer solution (7.5% w/v) was prepared, whereby PLGA (0.15 g), PLLA (0.05 g) and DOX were dissolved in DCM. Another polymer solution (0.35% w/v) containing PCPH (0.005g) and PTX was prepared. The theoretical loading of DOX and PTX were set at 20% w/w and 1% w/w, respectively. These two polymer solutions were mixed and ultra-sonicated for

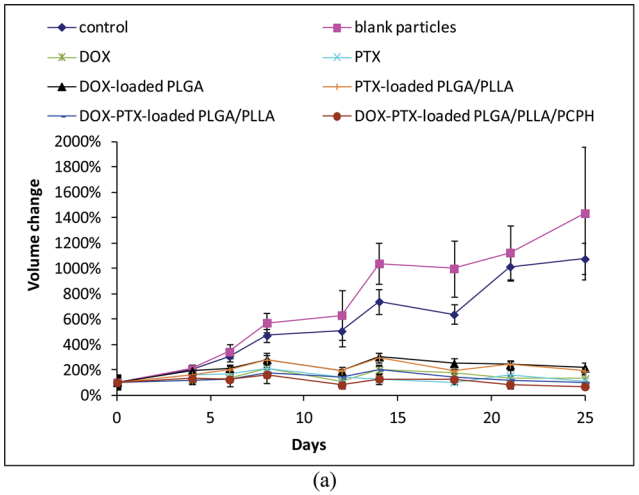

(a)

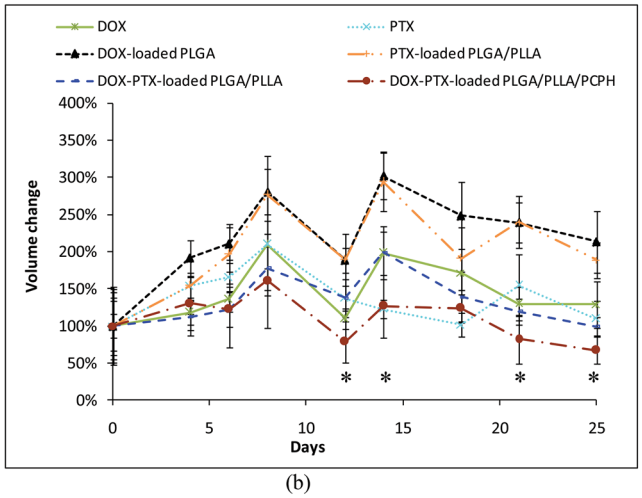

(b)

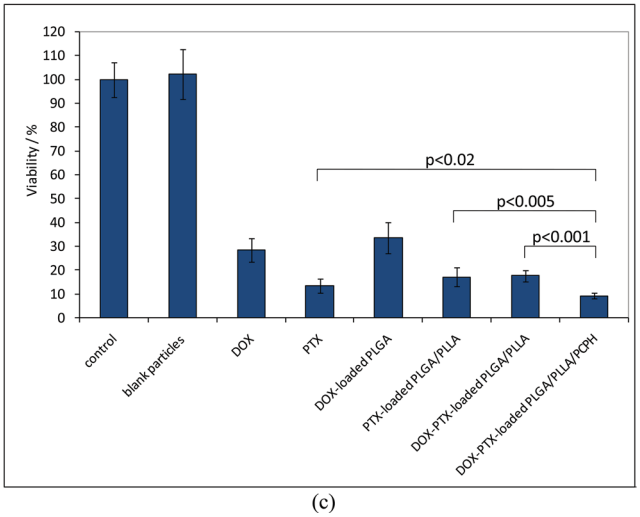

(c)

Figure 8. a) Growth monitoring of spheroids treated with free drug (DOX or PTX) or blank particles or single-drug-loaded microparticles or DOX-PTX-loaded microparticles over the course of study. b) A close-up of growth curve of spheroids treated with free drug or single-drug-loaded microparticles or DOX-PTX-loaded microparticles (*p < 0.05 for the comparison between DOX-PTX-loaded PLGA/PLLA and DOX-PTX-loaded PLGA/PLLA/PCPH microparticles). c) Viability of spheroids as assessed using the acid phosphatase assay at the end of study.

a min using an ultra-sonic processor (Sonic Vibra-Cell VC 130). After which, the homogenized polymer solution was poured into PVA aqueous solution (350 mL, 2% w/v). The emulsion was formed using an overhead stirrer (Calframo BDC1850–220) at 1600 rpm for 4 h at room temperature (25°C). The evaporation of DCM resulted in the phase separation of PLGA, PLLA and PCPH, yielding multilayered microparticles. Lastly, the particles were centrifuged, rinsed with deionized water, lyophilised and stored in a desiccator. For the fabrication of PLGA/PLLA microparticles, a similar method was employed but with different polymer masses (i.e., 0.3 g PLGA and 0.1 g PLLA) at 7.5% w/v. DOX and PTX were dissolved in PLGA/DCM solution and PLLA/DCM solution, respectively.

Morphological Analysis: The surface and internal morphologies of microparticles were analyzed using a scanning electron microscope (SEM, JEOL JSM-6360A) at 5 kV. The samples were submerged in liquid nitrogen before being cross-sectioned with a razor blade. Each sample was then coated with gold using a sputter coater (SPI-Module). For every sample batch, since particle morphologies were found to be consistent among at least ten microparticles, only one representative SEM micrograph is shown. Particle size was analyzed using the ImageJ software.

Determination of Polymer Distribution: Raman mapping was utilized to verify the polymer distribution within the microparticles. Microparticles that had been pre-sectioned were placed under a microscope objective with a laser power of up to approximately 20 mW. Raman point-by-point mapping measurements were performed in both the x and y directions using a Raman microscope (In-Via Reflex, Renishaw) equipped with a near-infrared enhanced deep depleted thermoelectrically Peltier-cooled CCD array detector (576×384 pixels) and a high-grade Leica microscope. The sample was irradiated with a 785-nm near-infrared diode laser, and an objective lens was used to collect the backscattered light. Measurement scans were collected using a static 1800-groove-per-mm dispersive grating in a spectral window from 300 to 1900 cm^{-1}, and the acquisition time for each spectrum was approximately 35 s. Raman mapping data were further analyzed using the band target entropy minimization (BTEM) algorithm to reconstruct pure component spectral estimates.[38]

Determination of Drug Distribution: The drug distribution within the microparticles loaded with dansyl chloride-tagged PTX and fluorescent DOX was examined using a confocal laser scanning microscope (CLSM, LSM710). A few droplets of the aqueous particle suspension were placed directly onto a microscope glass slide and sealed with a glass cover slip. The images were captured with 63×/1.40 oil objective lens, ×1 zoom and AxioCan MRm camera. Optical cross-sections were taken at various depths to determine drug distribution at the centerline of the microparticles. For dansyl chloride-tagged PTX (green), the excitation peak was centered at 405 nm, with an emission peak wavelength of 500 nm. For DOX (red), the excitation peak was centered at 488 nm, with an emission peak wavelength of 580 nm. The distinctive detection range for emission of each fluorophore allows the discrimination of possible overlapping emission of multiple fluorophores. These settings were used for all the samples to ensure consistency. Further analysis of the image was conducted using ZEN 2011 software.

NANO MICRO small

Drug Encapsulation Efficiency: Encapsulation efficiency is calculated by dividing the actual drug loading with theoretical drug loading within the microparticles. For DOX, microparticles (3 mg), in triplicate, were dissolved in DCM (1 mL). Upon complete dissolution, deionized water (10 mL) was added and the mixture was vortexed and left to phase separate. The DOX concentration in the aqueous layer was determined using an ultraviolet-visible (UV-vis) spectrophotometer (Shimadzu UV-2501) at 480 nm. For PTX, microparticles (3 mg), in triplicate, were first dissolved in DCM (1 mL). After which, ethanol (10 mL) was added to precipitate polymers.[39] The mixture was centrifuged and the supernatant was dried. ACN was then added to dissolve the solid PTX for UV-vis spectrophotometer analysis at 227 nm. A correction of the calculated encapsulation efficiency would be needed as inefficient extraction may exist. The same extraction procedure was carried out using blank particles and physical mixture of pure drug and blank particles. The extraction recovery efficiency was close to 90%.

In Vitro Drug Release: Drug-loaded microparticles (5 mg) were placed, in triplicate, in vials containing medium (5 mL) of PBS (pH 7.4) and Tween 80 (0.05%). The samples were incubated at 37 °C in a shaking incubator (50 rpm). At predetermined time points, the release medium (4 mL) from each sample was withdrawn and fresh medium (4 mL) was replenished to maintain sink condition. The concentration of DOX was directly analyzed using UV-vis spectrophotometer at 480 nm. PTX in the release medium was first extracted with DCM (4 mL). The extracted PTX was subsequently reconstituted with a known amount of ACN, after DCM had fully evaporated. The concentration of PTX was then determined by UV–vis spectrophotometer at 227 nm with proper background subtraction.[40–43] Background absorbance was subtracted using non-drug-loaded particles in the medium dealt with the same procedure mentioned above. Determination of the extraction efficiency was done by using known mass of pure PTX for the same extraction procedure. The determined extraction efficiency was ≈70%, and the released amount of PTX was corrected accordingly.

Hydrolytic Degradation: Microparticles (50 mg) were placed, in triplicate, in vials containing PBS/Tween 80 (50 mL) under moderate shaking and maintained at 37 °C. Microparticles were removed from the vials at predetermined time points, and rinsed with deionized water, followed by freeze-drying. Size-exclusion chromatography (SEC) (Agilent 1100 Series LC System) was used to determine the molecular weight of polymer, which was performed at 30 °C with chloroform as solvent, using a reflective index detector (RID), and the flow rate used was 1 mL min^{-1}. The polymers were separated by the THF dissolution method,[44] where PLGA is soluble in THF, while PLLA and PCPH are not. Microparticles (8 mg) were initially immersed in THF (1 mL) to dissolve the PLGA constituent. The PLLA/PCPH remnants and PLGA solution were subsequently separated by centrifugation. Afterwards, the oven-dried PLGA and PLLA/PCPH were dissolved separately in chloroform (1 mL), and tested with SEC. Since PCPH is not soluble in chloroform, filtering was done before performing SEC. Molecular weights of samples were obtained relative to the calibration curve using polystyrene standards.

Efficacy on 3D Spheroids: Magnetic MCF-7 spheroids (≈400 μm) were treated with free drug (DOX or PTX) or single-drug-loaded microparticles or DOX-PTX-loaded microparticles (at 2 μg mL^{-1} DOX and 0.4 μg mL^{-1} PTX). Equivalent amounts of free drugs corresponding to the amounts of drugs released from the particles (from in vitro release profiles) were administered. To facilitate imaging, the spheroids were separated from the microparticles through the use of a Transwell-96 Permeable Support with 3.0 μm pore polycarbonate membrane (Sigma CLS3385). Schematic representation of the Transwell setup is shown in the SI. The spheroids ($n = 6$) for each condition were incubated at 37 °C for 25 days. For free drug controls, DOX- and PTX-containing media were removed after 6 h incubation and fresh medium was replenished. For all the spheroids, culture media were changed every two days. Spheroid size was monitored by bright field microscopy by measuring the orthogonal diameters of each spheroid to calculate its volume. At the end of experiment, the acid phosphatase assay was performed to assess spheroid viability, as described in the SI.

Statistical Analysis: Data from different sets of particles were compared by unpaired Student's *t*-test and the one-way ANOVA analysis coupled with Tukey's multiple comparison tests. Statistically significant differences were verified when $p \leq 0.05$.

Supporting Information

Supporting Information is available from the Wiley Online Library or from the author.

Acknowledgements

*The authors would like to acknowledge financial support from the National Medical Research Council (NMRC) (NMRC/CIRG/1342/2012), the Agency for Science, Technology and Research (A*STAR) (Project No: 102 129 0098), the Biomedical Research Council, (BMRC, A*STAR), the Singapore Centre on Environmental Life Sciences Engineering (SCELSE) (M433C70000. M4220001.C70), the NTU NHG Ageing Research Grant (ARG/14012), and the School of Materials Science and Engineering (M020070110), Nanyang Technological University, Singapore. The authors would also like to thank Dr. Wang Xiujuan for her technical assistance in Raman mapping data acquisition. These acknowledgements were updated on October 15, 2014.*

[1] J. Lehár, A. S. Krueger, W. Avery, A. M. Heilbut, L. M. Johansen, E. R. Price, R. J. Rickles, G. F. Short Iii, J. E. Staunton, X. Jin, *Nat. Biotechnol.* **2009**, *27*, 659.
[2] W. G. Kaelin, *Nat. Rev. Cancer* **2005**, *5*, 689.
[3] F. Ahmed, R. I. Pakunlu, A. Brannan, F. Bates, T. Minko, D. E. Discher, *J. Controlled Release* **2006**, *116*, 150.
[4] L. Fan, F. Li, H. Zhang, Y. Wang, C. Cheng, X. Li, C.-h. Gu, Q. Yang, H. Wu, S. Zhang, *Biomaterials* **2010**, *31*, 5634.
[5] Y. Wang, S. Gao, W.-H. Ye, H. S. Yoon, Y.-Y. Yang, *Nat. Mater.* **2006**, *5*, 791.
[6] H. Wang, P. Zhao, W. Su, S. Wang, Z. Liao, R. Niu, J. Chang, *Biomaterials* **2010**, *31*, 8741.
[7] C. Zheng, M. Zheng, P. Gong, J. Deng, H. Yi, P. Zhang, Y. Zhang, P. Liu, Y. Ma, L. Cai, *Biomaterials* **2013**, *34*, 3431.
[8] X. Lu, Q.-Q. Wang, F.-J. Xu, G.-P. Tang, W.-T. Yang, *Biomaterials* **2011**, *32*, 4849.
[9] H. Wang, Y. Zhao, Y. Wu, Y.-l. Hu, K. Nan, G. Nie, H. Chen, *Biomaterials* **2011**, *32*, 8281.

[10] W. Tong, Y. Zhu, Z. Wang, C. Gao, H. Möhwald, *Macromol. Rapid Commun.* **2010**, *31*, 1015.
[11] M. Delcea, A. Yashchenok, K. Videnova, O. Kreft, H. Mohwald, A. G. Skirtach, *Macromol. Biosci.* **2010**, *10*, 465.
[12] Q. Xu, S. E. Chin, C.-H. Wang, D. W. Pack, *Biomaterials* **2013**, *34*, 3902.
[13] M. Shi, Y. Y. Yang, C. S. Chaw, S. H. Goh, S. M. Moochhala, S. Ng, J. Heller, *J. Controlled Release* **2003**, *89*, 167.
[14] D. L. Gustafson, A. L. Merz, M. E. Long, *Cancer Lett.* **2005**, *220*, 161.
[15] E. Briasoulis, V. Karavasilis, E. Tzamakou, D. Rammou, K. Soulti, C. Piperidou, N. Pavlidis, *Cancer. Chemother. Pharmacol.* **2004**, *53*, 452.
[16] B. A. Almond, A. R. Hadba, S. T. Freeman, B. J. Cuevas, A. M. York, C. J. Detrisac, E. P. Goldberg, *J. Controlled Release* **2003**, *91*, 147.
[17] C. Berkland, A. Cox, K. Kim, D. W. Pack, *J. Biomed. Mater. Res.* **2004**, *70A*, 576.
[18] R. Liggins, S. D'amours, J. Demetrick, L. Machan, H. Burt, *Biomaterials* **2000**, *21*, 1959.
[19] A. Loxley, B. Vincent, *J. Colloid Interface Sci.* **1998**, *208*, 49.
[20] E. C. Tan, R. Y. Lin, C. H. Wang, *J. Colloid Interface Sci.* **2005**, *291*, 135.
[21] A. Matsumoto, Y. Matsukawa, T. Suzuki, H. Yoshino, *J. Controlled Release* **2005**, *106*, 172.
[22] E. J. Pollauf, C. Berkland, K. K. Kim, D. W. Pack, *Int. J. Pharm.* **2005**, *301*, 294.
[23] A. J. Domb, *J. Polym. Sci. Part A: Polym. Chem.* **1993**, *31*, 1973.
[24] C. Berkland, E. Pollauf, D. W. Pack, K. Kim, *J. Controlled Release* **2004**, *96*, 101.
[25] W. L. Lee, E. Widjaja, S. C. J. Loo, *Small* **2010**, *6*, 1003.
[26] X. Huang, C. S. Brazel, *J. Controlled Release* **2001**, *73*, 121.
[27] M. J. Kipper, E. Shen, A. Determan, B. Narasimhan, *Biomaterials* **2002**, *23*, 4405.
[28] A. Sanchez, R. K. Gupta, M. J. Alonso, G. R. Siber, R. Langer, *J. Pharm. Sci.* **1996**, *85*, 547.
[29] H. K. Lee, J. H. Park, K. C. Kwon, *J. Controlled Release* **1997**, *44*, 283.
[30] T. L. Moore, S. W. Grimes, R. L. Lewis, F. Alexis, *Mol. Pharm.* **2013**, *11*, 276.
[31] V. H. Ho, W. M. Guo, C. L. Huang, S. F. Ho, S. Y. Chaw, E. Y. Tan, K. W. Ng, J. S. Loo, *Adv. Healthcare Mater.* **2013**, *2*, 1430.
[32] D. Lu, M. G. Wientjes, Z. Lu, J. L. -S. Au, *J. Pharmacol. Exp. Ther.* **2007**, *322*, 80.
[33] Z. Lu, M. Tsai, D. Lu, J. Wang, M. G. Wientjes, J. L. -S. Au, *J. Pharmacol. Exp. Ther.* **2008**, *327*, 673.
[34] R. M. Sutherland, *Science* **1988**, *240*, 177.
[35] I. Ojima, T. Inoue, S. Chakravarty, *J. Fluorine Chem.* **1999**, *97*, 3.
[36] T. T. Junttila, G. Li, K. Parsons, G. L. Phillips, M. X. Sliwkowski, *Breast Cancer Res. Treat.* **2011**, *128*, 347.
[37] T. M. Allen, P. R. Cullis, *Science* **2004**, *303*, 1818.
[38] E. Widjaja, W. L. Lee, S. C. J. Loo, *Anal. Chem.* **2010**, *82*, 1277.
[39] P. Perugini, I. Genta, B. Conti, T. Modena, D. Cocchi, D. Zaffe, F. Pavanetto, *Int. J. Pharm.* **2003**, *256*, 153.
[40] W. Peter Wuelfing, K. Kosuda, A. C. Templeton, A. Harman, M. D. Mowery, R. A. Reed, *J. Pharm. Biomed. Anal.* **2006**, *41*, 774.
[41] M. J. Heslinga, E. M. Mastria, O. Eniola-Adefeso, *J. Controlled Release* **2009**, *138*, 235.
[42] X. Xu, P. Lu, M. Guo, M. Fang, *Appl. Surf. Sci.* **2010**, *256*, 2367.
[43] Y. H. Yu, E. Kim, D. E. Park, G. Shim, S. Lee, Y. B. Kim, C.-W. Kim, Y.-K. Oh, *Eur. J. Pharm. Biopharm.* **2012**, *80*, 268.
[44] W. L. Lee, P. Yu, M. Hong, E. Widjaja, S. C. J. Loo, *Acta Biomater.* **2012**, *8*, 2271.

Received: February 26, 2014
Published online: June 20, 2014

